

# Journal of Materials Chemistry A

Accepted Manuscript



This is an *Accepted Manuscript*, which has been through the Royal Society of Chemistry peer review process and has been accepted for publication.

*Accepted Manuscripts* are published online shortly after acceptance, before technical editing, formatting and proof reading. Using this free service, authors can make their results available to the community, in citable form, before we publish the edited article. We will replace this *Accepted Manuscript* with the edited and formatted *Advance Article* as soon as it is available.

You can find more information about *Accepted Manuscripts* in the [Information for Authors](#).

Please note that technical editing may introduce minor changes to the text and/or graphics, which may alter content. The journal's standard [Terms & Conditions](#) and the [Ethical guidelines](#) still apply. In no event shall the Royal Society of Chemistry be held responsible for any errors or omissions in this *Accepted Manuscript* or any consequences arising from the use of any information it contains.

# Stable Layered P3/P2 Na<sub>0.66</sub>Co<sub>0.5</sub>Mn<sub>0.5</sub>O<sub>2</sub> Cathode Materials for Sodium Ion Batteries

Xiaoqing Chen, Xianlong Zhou, Meng Hu, Jing Liang, Dihua Wu, Jinping Wei,\* Zhen Zhou\*

Received (in XXX, XXX) Xth XXXXXXXXXX 20XX, Accepted Xth XXXXXXXXXX 20XX

DOI: 10.1039/b000000x

Rechargeable sodium ion batteries are promising for next-generation energy storage devices due to the low cost and rich natural abundance of Na. However, it is still a large challenge to suppress the phase change of cathode materials in the high-voltage region. Unlike P-type single phase composites, here, we tactfully present a facile strategy to prepare P3/P2-type biphasic layered Na<sub>0.66</sub>Mn<sub>0.5</sub>Co<sub>0.5</sub>O<sub>2</sub>, namely, integrating P2 into P3 layered materials. The crystalline structure of Na<sub>0.66</sub>Co<sub>0.5</sub>Mn<sub>0.5</sub>O<sub>2</sub>, investigated by ex-situ X-ray diffraction, was well maintained over long cycles in a high-voltage range. Taking advantage of structural stabilization, Na<sub>0.66</sub>Mn<sub>0.5</sub>Co<sub>0.5</sub>O<sub>2</sub> cathode materials displayed remarkably steady discharge capacity at high rates. With outstanding structural flexibility and electrochemical performances, Na<sub>0.66</sub>Co<sub>0.5</sub>Mn<sub>0.5</sub>O<sub>2</sub> would stimulate the development of sodium-ion batteries.

## 1. Introduction

Presently, due to the massive consumption of fossil fuels and hostile environment pollutions, the wide application of sustainable energy has been accelerated in light of achieving the need for cleaner energy sources. For this purpose, lithium ion batteries, with high energy and power density among all secondary battery technologies, have been considered as one of the most indispensable devices for electrical energy storage.<sup>1,2</sup> However, with the uninterruptedly increasing demand of portable electronics, electric vehicles and smart grids, the high cost and limited resource of lithium have constrained the large-scale supply of lithium ion batteries.<sup>3,4</sup> As a consequence, it is very critical to develop an alternative for next-generation energy storage systems. In sharp contrast, ambient temperature sodium-ion batteries show obvious advantage owing to the much richer worldwide abundance and the lower price of Na than those of Li. Na also has similar electrochemical properties to Li because they are located at the same main group in the periodic table.<sup>5</sup>

Investigations on Na ion batteries have increased dramatically in the past years.<sup>6-8</sup> Although much progress has been made, the electrochemical performance of Na ion batteries is still inferior compared with Li ion batteries. Learning from the development of Li ion batteries, researchers have transferred more attention to multiple layered Na<sub>x</sub>MO<sub>2</sub> (M = transition metals, such as Mn and Co).<sup>9-14</sup> Sodium-based layered materials can be classified into two major groups: P-type (prismatic sites) and O-type (octahedral sites), in accordance with the alkali-ion interaction occupation.<sup>15</sup> Up to date, the unitary compounds containing only one transition metal in the repeating (MO<sub>2</sub>)<sub>n</sub> sheets, such as Na<sub>x</sub>CrO<sub>2</sub>,<sup>16</sup> Na<sub>x</sub>VO<sub>2</sub>,<sup>17</sup> and Na<sub>x</sub>CoO<sub>2</sub>,<sup>18</sup> were intensively investigated in the early years. Nevertheless, they delivered limited capacity and poor rate capability, probably due to multiple phase changes during charge/discharge processes. Substituted sectional

transition metals, namely, binary and ternary ramifications, have been used to improve the structural stability and electrochemical performance, such as Na<sub>x</sub>Co<sub>1/2</sub>Fe<sub>1/2</sub>O<sub>2</sub>,<sup>19</sup> Na<sub>x</sub>Fe<sub>1/2</sub>Mn<sub>1/2</sub>O<sub>2</sub>,<sup>20</sup> Na<sub>x</sub>Ni<sub>1/3</sub>Co<sub>1/3</sub>Fe<sub>1/3</sub>O<sub>2</sub>,<sup>21</sup> and Na[Ni<sub>0.4</sub>Fe<sub>0.2</sub>Mn<sub>0.4-x</sub>Ti<sub>x</sub>]O<sub>2</sub>.<sup>22</sup>

Currently, sodium-based layered oxides consist of various structures, including P2, P3, and O3, which is mainly connected with calcination temperatures, stoichiometric ratios of sodium in the compounds and preparation methods.<sup>23,24</sup> Sathiyaraj et al. reported pure O3-type NaNi<sub>1/3</sub>Mn<sub>1/3</sub>Co<sub>1/3</sub>O<sub>2</sub> with a capacity of 120 mAh g<sup>-1</sup> in the voltage region of 2-3.75 V, and further investigated phase evolution with in-situ X-ray diffraction (XRD) during Na-ion insertion and extraction processes.<sup>25</sup> Nowadays, P-type layered oxides, regarded as promising candidates for sodium-ion batteries, have aroused more interest due to their superior electrochemical performances. Wang et al. performed detailed studies on the electrochemical performances of P2-Na<sub>2/3</sub>Mn<sub>y</sub>Co<sub>1-y</sub>O<sub>2</sub> composites prepared through conventional solid state reactions; however, it only exhibited 123 mAhg<sup>-1</sup> even at a low rate (0.1 C).<sup>26</sup> In addition, these Na-based oxides undergo phase transformation in the high-voltage region. Meng and co-workers demonstrated that the significant capacity fading and poor rate capability are affected by the P2-O2 phase change occurring higher than 4.2 V.<sup>27</sup> The limited capacity and structure instability cannot compete with other available cathode materials for Na ion batteries, and meet the demand in practical applications. Hence, there still remains a huge challenge for Na ion batteries to find cathode materials with both high capacity and good rate capability.

Very recently, Johnson et al. have successfully introduced multiphase (P2/O3) material that leads to an unexpected enhancement of both specific capacity and rate capability.<sup>14</sup> In comparison, Chagas et al. have reported P2/P3 mixed layered materials, and interestingly Na<sub>x</sub>Ni<sub>0.22</sub>Co<sub>0.12</sub>Mn<sub>0.66</sub>O<sub>2</sub> exhibited an

available capacity of  $\sim 146.8$  mAh  $g^{-1}$  in the voltage range of 2.1 to 4.3 V at 0.1 C rate,<sup>24</sup> whereas the inferior rate performances restrict its wide applications. On this basis of the ideas mentioned above, we present a simple strategy to fabricate P3/P2-type biphas layered  $Na_{0.66}Mn_{0.5}Co_{0.5}O_2$ . It demonstrated outstanding electrochemical performance in terms of high capacity of 156.1 mAh  $g^{-1}$  at 1 C. Furthermore, it exhibited significant improvement in high-rate capability and long-term cycling stability compared with those already reported in the literature.

## 2. Experimental Section

### Material Preparation

P3/P2 biphas  $Na_{0.66}[Mn_{1/2}Co_{1/2}]O_2$  was prepared through a conventional sol-gel route from stoichiometric amounts of NaAc,  $Mn(Ac)_2 \cdot 4H_2O$  and  $Co(Ac)_2 \cdot 4H_2O$  (Sigma Aldrich) in the proportion of 4:3:3 with excessive 5% sodium sources. The stoichiometric precursors were mixed with citric acid (chelating agent) in deionized water, and form a pink aqueous solution. In order to obtain the colloidal sol, the solution was kept at 80°C under constant agitation, and then the achieved sol was dried overnight at 100°C in air. The resulting powders were firstly annealed in air at 500°C for 6 h. After cooling to room temperature, the powders were ground again and calcined at 800°C for 15 h in air to gain layered oxides. P3-type  $Na_{0.66}[Mn_{1/2}Co_{1/2}]O_2$  was prepared under the same condition except calcination at 700°C in air for 15 h. Finally, the sample was ground and stored in an Ar-filled glove box for further use.

### Material Characterization

XRD patterns of the samples were conducted with Cu  $K\alpha$  radiation in the  $2\theta$  range from 10° to 70° by using a D/Max III diffractometer. The site occupation of ions was calculated through Rietveld refinement of the XRD patterns with General

Structure Analysis System (GSAS) program. The morphology and microstructure of the samples were observed through field emission scanning electron microscope (FESEM, JEOL-JSM7500) and transmission electron microscope (TEM) (FEI Tecnai G2F-20 field emission TEM). X-ray photoelectron spectroscopy (XPS, Axis Ultra DLD, Kratos Analytical) was performed to obtain oxidation states of transition metals. The sodium and transition metal ratios in the samples were detected by inductively coupled plasma-atomic emission spectroscopy (ICP-AES, ICP-9000(N+M), Thermo Jarrell-Ash Corp, USA).

### Electrochemical Tests

A slurry was obtained by mixing active material (70wt%), acetylene black (20wt%), polyvinylidene fluoride (PVDF, 10wt%) and appropriate amount of N-methyl-2-pyrrolidone (NMP), and the slurry was pasted on aluminum foil collector and dried at 80°C for 12 h in air. Disk cathodes were punched and pressed with a diameter of 1.2 cm and mass loading of  $\sim 0.9$  mg/cm<sup>2</sup>. Sodium metal was used as the anode. The electrolyte was 1.0 mol/L  $NaClO_4$  in ethylene carbonate/propylene carbonate (EC/PC, 1:1, v/v), and glass fibers were used as separators. CR2025-type coin cells were assembled in an Ar-filled glove box, and the cells were then cycled at different rates between 1.5 and 4.3 V on a LAND CT2001 battery cycler at 25°C. Cyclic voltammetric (CV) measurements were performed at a scan rate of 0.1 mVs<sup>-1</sup> on a CHI600A electrochemical workstation (Shanghai Chenhua). Electrochemical impedance spectroscopy (EIS) was conducted on a Zahner-Elektrik IM6e electrochemical workstation with the frequency region from 100 kHz to 10 mHz and an AC signal of 5 mV in amplitude as the sine perturbation. All the above measurements were conducted at room temperature.

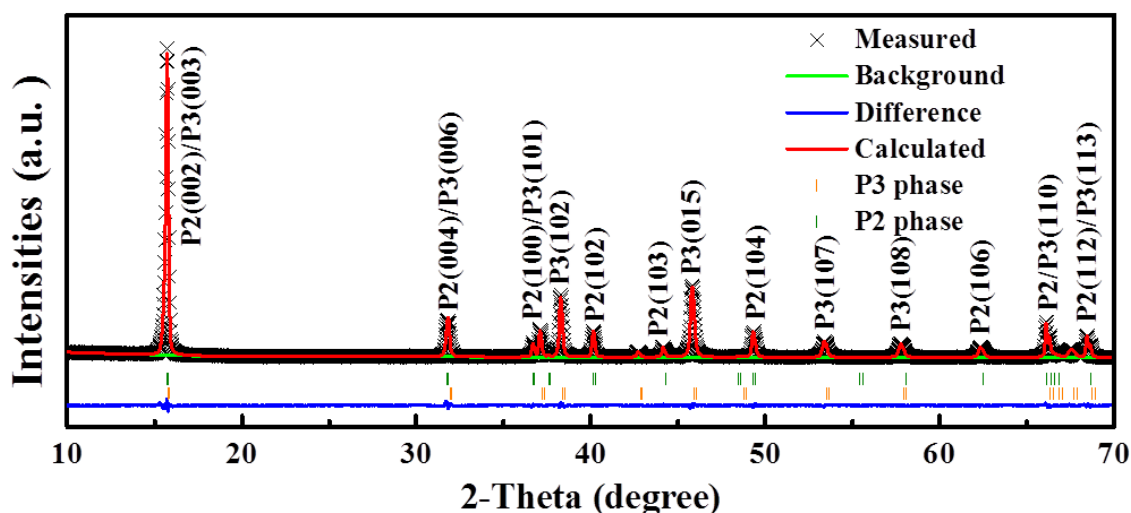


**Fig. 1** Observed and calculated XRD profiles for  $Na_{0.66}Mn_{0.5}Co_{0.5}O_2$ : the experimental data (black ×'s), calculated pattern (red line), Bragg positions (green and orange bars) and difference curves (blue line).

### 3. Results and discussion

Initially, through the ICP-AES analysis, the ratio of Na, Mn and Co was 0.62, 0.51 and 0.49, respectively, and it was very close to the designed value ( $\text{Na}_{0.66}\text{Mn}_{0.5}\text{Co}_{0.5}\text{O}_2$ ) with partial evaporation of Na. The prepared sample was then studied by XRD, and the patterns and corresponding Rietveld analysis are shown in Fig. 1. The XRD patterns clearly show that  $\text{Na}_{0.66}\text{Co}_{0.5}\text{Mn}_{0.5}\text{O}_2$  consists of a mixture of P2-type (space group: P63/mmc) and P3-type (space group: R3m) structures.<sup>28</sup> For comparison, the XRD patterns of P3-phase  $\text{Na}_{0.66}\text{Co}_{0.5}\text{Mn}_{0.5}\text{O}_2$  are shown in Fig. S1 (ESI). A noticeable feature in the Rietveld XRD patterns is that the diffraction lines of P3-phase are much stronger than those of P2-phase, which can also be illustrated from the Rietveld ratio (P3: 76.05wt%, P2: 23.95wt%). As shown in Table 1, the Rietveld refined lattice parameters for P-type mixed samples are  $a = 2.81466 \text{ \AA}$  and  $c = 16.78169 \text{ \AA}$  for the P3-component and  $a = 2.82319 \text{ \AA}$  and  $c = 11.25026 \text{ \AA}$  for the P2-component (Rwp = 7.1% and Rp = 4.74%). More details (cell parameters and atomic position) about the Rietveld refinement are depicted in Table S1 (ESI). The schematic illustration of the biphas (P2 and P3) structures can be found in Fig. 2.

In order to determine the oxidation state of transition metals

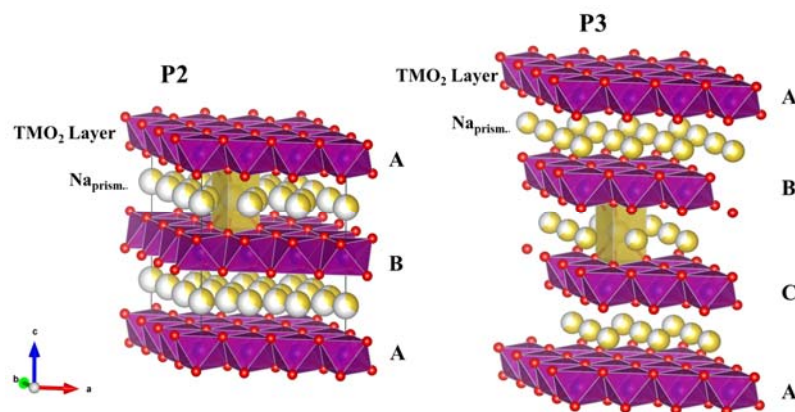


Fig. 2 Layered structures of P2 (left) and P3 (right).

Table 1. Crystallographic parameters obtained from Rietveld refinement.

Phase	Space group	Lattice parameters	wt%
P3	R3m	$a = 2.81466 \text{ \AA}$ $c = 16.78169 \text{ \AA}$	76.05%
P2	P63/mmc	$a = 2.82319 \text{ \AA}$ $c = 11.25026 \text{ \AA}$	23.95%

The size and morphology of the as-prepared samples were investigated by SEM and TEM. As shown in Fig. 4, the samples appear as uniformly distributed particles but with partly agglomeration. Apparently, the particles show typical hexagonal-like shape with the particle size between 300 and 400 nm. The element mapping is shown in Fig. S2, and it reveals that Na, Mn, Co and O are uniformly distributed in the particles.

in the sample, XPS was performed. The observed Co and Mn2p peaks are shown in Fig. 3a and 3b, respectively. In the Co2p spectrum, the two peaks can be assigned to  $\text{Co}2p_{1/2}$  at 795.1 eV and  $\text{Co}2p_{3/2}$  at 780.0 eV. The resulting binding energies deduced that the valence of Co is +3.<sup>29</sup> In Fig. 3b the two core peaks located at 654.1 eV and 642.0 eV can be ascribed to tetravalent Mn.<sup>30,31</sup> The oxidation states of the transition metals are in good agreement with the demonstrated material.<sup>32</sup> However, there is a little difference between the experimental and theoretical data of the oxidation state of Mn. The layered sodium oxide was prepared at high temperature, especially calcined for 15 hours in air, and this will lead to partial sodium evaporated, corresponding to the increased valence state of Mn. In addition, it has been reported that the P-type layered cathode material will uptake  $\text{H}_2\text{O}$ ,  $\text{CO}_2$ , and  $\text{O}_2$  in air, concomitant with oxidation of Mn(III) to Mn(IV).<sup>33</sup> Although our prepared samples were stored in an Ar-filled glove box, the samples had to be exposed in air during XPS tests. Under this condition, Mn(III) will be easily oxidized to Mn(IV). Therefore, we think that Mn(IV) may exist in the solid surface.

Electrochemical behaviors of the biphas layered  $\text{Na}_{0.66}\text{Mn}_{0.5}\text{Co}_{0.5}\text{O}_2$  were characterized by CV and galvanostatic charge/discharge cycling. Fig. S3 shows the CV curves of the  $\text{Na}_{0.66}\text{Mn}_{0.5}\text{Co}_{0.5}\text{O}_2$  electrode. There are two pairs of redox peaks, the anodic peaks at 2.25 V and 4.0 V, and the cathodic peaks at 1.75 V and 3.75 V, corresponding to  $\text{Mn}^{4+}/\text{Mn}^{3+}$  and  $\text{Co}^{3+}/\text{Co}^{2+}$  couples, respectively. Neither the profile nor the location of the

peaks changes much upon consecutive cycles, indicating its high structural stability during  $\text{Na}^+$  intercalation/deintercalation processes. Fig. 5 shows the voltage profiles and cycling behaviors of the  $\text{Na}_{0.66}\text{Mn}_{0.5}\text{Co}_{0.5}\text{O}_2$  electrode at various rates. In accordance with the CV curves, the  $\text{Na}_{0.66}\text{Mn}_{0.5}\text{Co}_{0.5}\text{O}_2$  electrodes exhibited two discharge plateaus at 3.75 and 2.25 V. All curves generally depict similar characteristics, probably ascribed to the stabilized layered structure. Until now, most of the reported layered cathode materials are lack of high-rate performance and long cycle life due to the larger radius of  $\text{Na}^+$  than that of  $\text{Li}^+$ .<sup>24,34,35</sup> However, the biphasic  $\text{Na}_{0.66}\text{Mn}_{0.5}\text{Co}_{0.5}\text{O}_2$  cathode delivered discharge capacities of 156.1, 141.8 and 126.6 mAh  $\text{g}^{-1}$

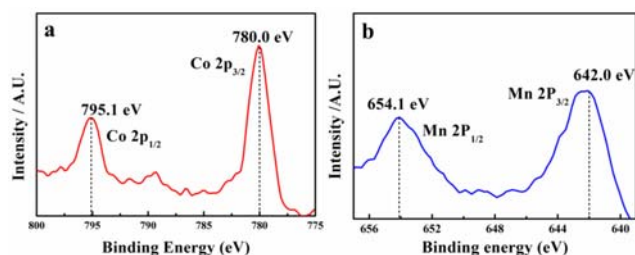


**Fig. 3** XPS of the as-prepared sample: (a) Co2p and (b) Mn2p core levels.

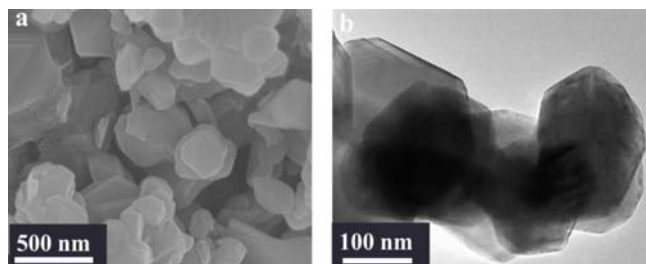


**Fig. 4** (a) SEM and (b) TEM images of the prepared sample.

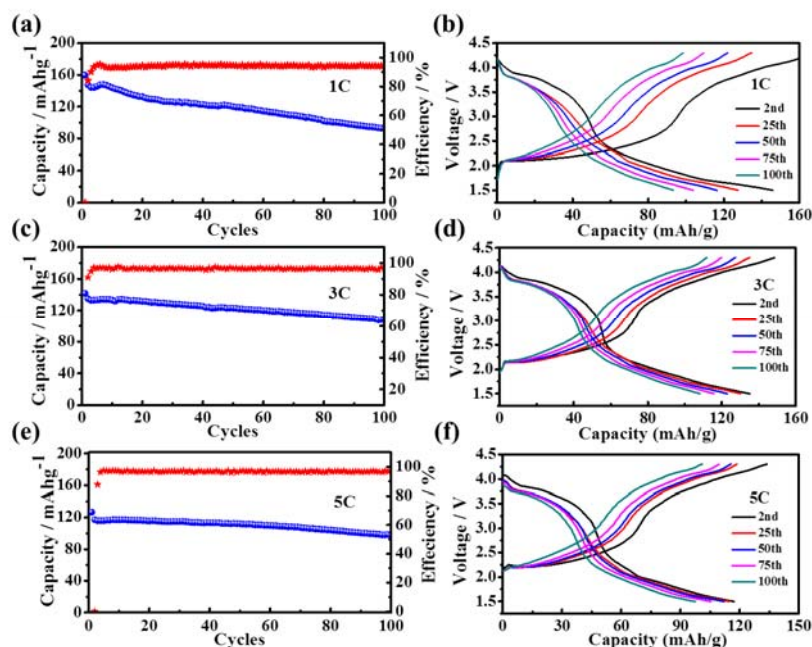


**Fig. 5** Electrochemical performances of coin cells with  $\text{Na}_{0.66}\text{Mn}_{0.5}\text{Co}_{0.5}\text{O}_2$  cathodes upon galvanostatic charge-discharge cycles in the range of 1.5-4.3 V. (a,c,e) Cycling performances and (b,d,f) charge/discharge curves at 1 C, 3 C and 5 C, respectively.

with an increased columbic efficiency from 1 C to 5 C, respectively, as shown in Fig. 5. Importantly, the electrochemical performance of the P2/P3 biphasic  $\text{Na}_{0.66}\text{Mn}_{0.5}\text{Co}_{0.5}\text{O}_2$  was highly improved compared with the pure P3 phase  $\text{Na}_{0.66}\text{Mn}_{0.5}\text{Co}_{0.5}\text{O}_2$  (Figs. S4 and S5). More remarkably, even at the high rate of 5 C, the reversible capacity of the P2/P3 biphasic  $\text{Na}_{0.66}\text{Mn}_{0.5}\text{Co}_{0.5}\text{O}_2$  still reached 97.5 mAh  $\text{g}^{-1}$ , corresponding to capacity retention of 77% after 100 cycles. Yoshida et al.<sup>12</sup> reported that P2-type  $\text{Na}_{2/3}\text{Ni}_{1/3}\text{Mn}_{5/6}\text{Ti}_{1/6}\text{O}_2$  showed superior cyclability to  $\text{Na}_{2/3}\text{Ni}_{1/3}\text{Mn}_{2/3}\text{O}_2$ . Nevertheless, low discharge capacity of 127 mAh  $\text{g}^{-1}$  was observed when the material was cycled in the range of 2.5-4.5 V at a rate of C/20 (1 C=241 mAh  $\text{g}^{-1}$ ). Chagas et al.<sup>24</sup> proposed the P2/P3 mixed phase  $\text{Na}_x\text{Ni}_{0.22}\text{Co}_{0.11}\text{Mn}_{0.66}\text{O}_2$  electrode, while it demonstrated only ~53 mAh  $\text{g}^{-1}$  at 5 C (651 mAh  $\text{g}^{-1}$ ). Compared with the layered cathode materials reported so far, our samples showed more excellent cyclic stability and high rate capability, which is related to the structure stability of the biphasic  $\text{Na}_{0.66}\text{Mn}_{0.5}\text{Co}_{0.5}\text{O}_2$  cathode materials.

In terms of the electrochemical and structural reversibility, the higher rate charge/discharge cycling performance of biphasic  $\text{Na}_{0.66}\text{Mn}_{0.5}\text{Co}_{0.5}\text{O}_2$  was further investigated in the voltage range of 1.5 to 4.3 V. As shown in Fig. 6b, the  $\text{Na}_{0.66}\text{Mn}_{0.5}\text{Co}_{0.5}\text{O}_2$  electrode displayed remarkably steady discharge capacity from initial 86.5 mAh  $\text{g}^{-1}$  to 78.9 mAh  $\text{g}^{-1}$  at the 100<sup>th</sup> cycle tested at 10 C, with high capacity retention of 91%. Even cycled at 20 C, the  $\text{Na}_{0.66}\text{Mn}_{0.5}\text{Co}_{0.5}\text{O}_2$  cathode still remained 84.5% of its initial discharge capacity after 100 cycles (from 67.0 mAh  $\text{g}^{-1}$  to 56.6 mAh  $\text{g}^{-1}$ ). Consequently, the mixing of P-type phases could endow layered sodium oxides with outstanding discharge capacity and rate performance.

The phase transition of biphasic  $\text{Na}_{0.66}\text{Mn}_{0.5}\text{Co}_{0.5}\text{O}_2$  electrodes upon cycling is closely related to the cycling stability of this material.<sup>36</sup> To elucidate the structural evolution of  $\text{Na}_{0.66}\text{Mn}_{0.5}\text{Co}_{0.5}\text{O}_2$  cathodes, ex-situ XRD was conducted at 5 different depths of charge and discharge during  $\text{Na}^+$  insertion/extraction processes, as shown in Fig. 7. Upon the sodiation/desodiation processes, all the diffraction patterns change hardly except the peak position. Detailed comparison of peak shift could be found in Fig. 7c, corresponding to the 10 magnified selective patterns in the range of 11-35° and 42.5-54°.

Jung et al.<sup>37</sup> reported that  $\text{P2-Na}_{0.7}\text{Fe}_{0.4}\text{Mn}_{0.4}\text{Co}_{0.2}\text{O}_2$  cathode material transformed from P2 to O2 after it was charged to 4.1 V, and Dahn et al.<sup>38</sup> demonstrated that the (10 $l$ ) peaks became

broader as the O2 phase appeared. Compared with the reported 15 results, the (10 $l$ ) diffraction peaks of the P2/P3 biphasic, such as the (104) peak at ~49°, slightly shift to the lower angles upon  $\text{Na}^+$  extraction, but the peaks for sodiation process reversibly return to the original position on the contrary. Recently, Li et al.<sup>39</sup> have also certified that the structure of  $\text{P2-Na}_{7/9}\text{Cu}_{2/9}\text{Fe}_{1/9}\text{Mn}_{2/3}\text{O}_2$  is 20 electrochemically stable, with only some gradual shift of the peak position upon  $\text{Na}^+$  extraction/insertion process even with the high cutoff voltage of 4.2 V. Furthermore, the XRD patterns of the  $\text{Na}_{0.66}\text{Mn}_{0.5}\text{Co}_{0.5}\text{O}_2$  electrode tested after 10 and 100 cycles at 5 C match well with those of the pristine one (Fig. S6). Apparently, 25 this demonstrates the structural stabilization of biphasic  $\text{Na}_{0.66}\text{Mn}_{0.5}\text{Co}_{0.5}\text{O}_2$  during Na-ion insertion/extraction at high rate.

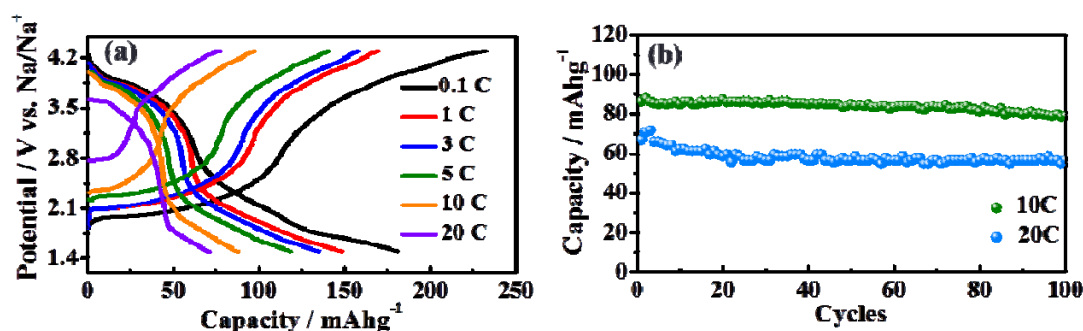


Fig. 6 (a) Rate capability (1 C = 170 mAhg<sup>-1</sup>) and (b) Cycling performance at 10 C and 20 C for 100 cycles of  $\text{Na}_{0.66}\text{Mn}_{0.5}\text{Co}_{0.5}\text{O}_2$  electrodes.

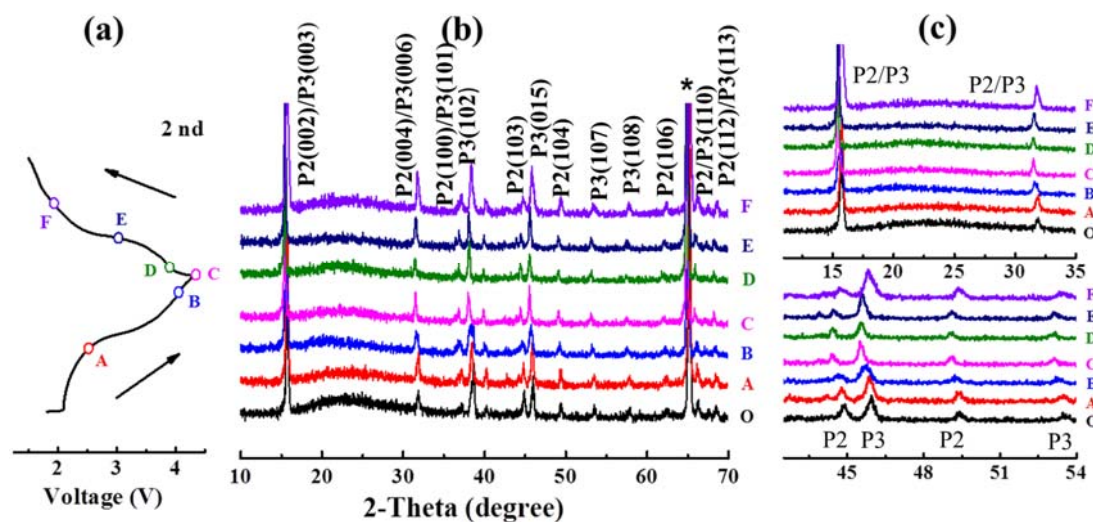
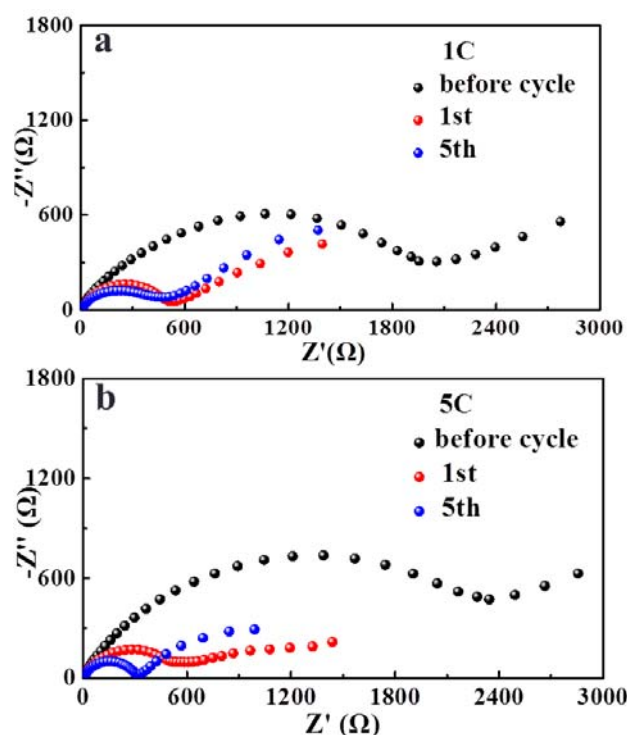


Fig. 7 (a) Charge/discharge profiles of the  $\text{Na}_{0.66}\text{Mn}_{0.5}\text{Co}_{0.5}\text{O}_2$  electrodes tested at 1 C rate for the second cycle, the letters A-F stand for the depths of charge/discharge at which the cathodes were recorded by ex-situ XRD. (b) XRD patterns of the electrode at various states. The asterisk is the characteristic diffraction peaks of Al foils. (c) The corresponding magnified XRD patterns (The letter O was taken for the pristine electrode).



**Fig. 8** EIS evolution of the  $\text{Na}_{0.66}\text{Mn}_{0.5}\text{Co}_{0.5}\text{O}_2$  electrode under various rates.

#### 4. Conclusions

In summary, we have prepared a potential cathode material,  $\text{Na}_{0.66}\text{Co}_{0.5}\text{Mn}_{0.5}\text{O}_2$ , for Na-ion batteries, which was characterized as a well-defined P3/P2-type biphasic structure. The as-prepared  $\text{Na}_{0.66}\text{Mn}_{0.5}\text{Co}_{0.5}\text{O}_2$  electrode exhibited a high discharge capacity of  $156.1 \text{ mAh g}^{-1}$  at 1 C in the voltage range of 1.5–4.3 V. In addition, our  $\text{Na}_{0.66}\text{Mn}_{0.5}\text{Co}_{0.5}\text{O}_2$  electrodes delivered available discharge capacity of  $78.9 \text{ mAh g}^{-1}$  and good capacity retention (91%) after 100 cycles at 10 C. Even at a higher rate (20 C), the  $\text{Na}_{0.66}\text{Mn}_{0.5}\text{Co}_{0.5}\text{O}_2$  cathodes still remained 84.5% of its initial discharge capacity over 100 cycles (from  $67.0 \text{ mAh g}^{-1}$  to  $56.6 \text{ mAh g}^{-1}$ ). More importantly, the crystal structure of  $\text{Na}_{0.66}\text{Mn}_{0.5}\text{Co}_{0.5}\text{O}_2$  after cycles, investigated by ex-XRD, matched well with that of the pristine one. In consequence, the P3/P2-type layered oxide materials are effective alternatives for sodium-ion batteries in term of excellent electrochemical performances.

#### 5. Acknowledgements

This work was supported by NSFC (21421001) and MOE Innovation Team (IRT13022) in China.

Key Laboratory of Advanced Energy Materials Chemistry (Ministry of Education), Institute of New Energy Material Chemistry, Collaborative Innovation Center of Chemical Science and Engineering (Tianjin), School of Materials Science and Engineering, National Institute of Advanced Materials, Nankai University, Tianjin 300071, P.R. China  
Email: [jpwei@nankai.edu.cn](mailto:jpwei@nankai.edu.cn); [zhouzhen@nankai.edu.cn](mailto:zhouzhen@nankai.edu.cn)

† Electronic supplementary information (ESI) available: More materials characterizations and electrochemical tests. See DOI: 10.1039/c0xx00000x

#### Notes and references

- J. M. Tarascon and M. Armand, *Nature*, 2001, **414**, 359–367.
- J. B. Goodenough and Y. Kim, *Chem. Mater.*, 2010, **22**, 587–603.
- J. Kim, H. D. Lim, H. Gwon and K. Kang, *Phys. Chem. Chem. Phys.*, 2013, **15**, 3623–3629.
- X. Zhou, Y. Zhong, M. Yang, M. Hu, J. Wei and Z. Zhou, *Chem. Commun.*, 2014, **50**, 12888–128891.
- V. Palomares, M. Casas-Cabanas, E. Castillo-Martinez, M. H. Han and T. Rojo, *Energy Environ. Sci.*, 2013, **6**, 2312–2337.
- J. Molenda, C. Delmas and P. Hagenmuller, *Solid State Ionics*, 1983, **9–10**, 431–435.
- J. M. Tarascon and G. W. Hull, *Solid State Ionics*, 1986, **22**, 85–96.
- K. West, B. Zachau-Christiansen, T. Jacobsen and S. Skaarup, *Solid State Ionics*, 1988, **28–30**, 1128–1131.
- S.-M. Oh, S.-T. Myung, J.-Y. Hwang, B. Scrosati, K. Amine and Y.-K. Sun, *Chem. Mater.*, 2014, **26**, 6165–6171.
- S. Kalluri, K. H. Seng, W. K. Pang, Z. Guo, Z. Chen, H. K. Liu and S. X. Dou, *ACS Appl. Mater. Interfaces*, 2014, **6**, 8953–8958.

To make clear why the biphasic  $\text{Na}_{0.66}\text{Mn}_{0.5}\text{Co}_{0.5}\text{O}_2$  layered cathode materials have the outstanding rate capability and long-term cyclability, EIS was conducted on the electrode upon the charge/discharge process at various rates. Fig. 8 presents the Nyquist plots of the cells tested at 1 C and 5 C before and after 10 cycling. They are composed of a single semicircle in the high frequency region and a slope at the low frequency region. In all Nyquist plots, the diameter of the semicircle at the high frequency region stands for the charge transfer resistance ( $R_{ct}$ ) and the slope in the low frequency is the Warburg impedance, which is associated with the sodium-ion diffusion in the electrode. Obviously, after the first cycle, the  $R_{ct}$  of the electrode at different rates decreased to some extent. Although the  $R_{ct}$  values still continued to decline after 5 cycles, the  $R_{ct}$  measured at 5 C decreases more steeply than that at 1 C. The decrease of  $R_{ct}$  after the 1st cycle resulted from the fact that the electrolyte penetrated gradually into the  $\text{Na}_{0.66}\text{Mn}_{0.5}\text{Co}_{0.5}\text{O}_2$  electrode. Furthermore, there are lower  $R_{ct}$  values after cycles at 5 C than at 1 C, probably due to more reactions between active materials and electrolytes at lower rates, especially at high cutoff voltages.<sup>40,41</sup> These results were further verified by contrasting the EIS between 5 C and 0.1 C at the same stage (Fig. S7). Also, we performed EIS tests to demonstrate that the P3/P2 biphasic has advantages in cyclability and high-rate capability than the pure P3 phase (Fig. S8). Obviously, the P3/P2 biphasic shows much smaller  $R_{ct}$  values than that of pure P3 phase under each testing condition, corresponding to easier sodiation/desodiation during the electrochemical process in the biphasic system.

11. M. Tamaru, X. Wang, M. Okubo and A. Yamada, *Electrochem. Commun.*, 2013, **33**, 23-26.
12. H. Yoshida, N. Yabuuchi, K. Kubota, I. Ikeuchi, A. Garsuch, M. Schulz-Dobrick and S. Komaba, *Chem. Commun.*, 2014, **50**, 3677-3680.
13. J.-J. Ding, Y.-N. Zhou, Q. Sun and Z.-W. Fu, *Electrochem. Commun.*, 2012, **22**, 85-88.
14. E. Lee, J. Lu, Y. Ren, X. Luo, X. Zhang, J. Wen, D. Miller, A. DeWahl, S. Hackney, B. Key, D. Kim, M. D. Slater and C. S. Johnson, *Adv. Energy Mater.*, 2014, **4**, 1-8.
15. C. Delmas, C. Fouassier and P. Hagemuller, *Physica B+C*, 1980, **99**, 81-85.
16. S. Komaba, C. Takei, T. Nakayama, A. Ogata and N. Yabuuchi, *Electrochem. Commun.*, 2010, **12**, 355-358.
17. C. Didier, M. Guignard, C. Denage, O. Szajwaj, S. Ito, I. Saadoune, J. Darriet and C. Delmas, *Electrochem. Solid-State Lett.*, 2011, **14**, 75-78.
18. R. Berthelot, D. Carlier and C. Delmas, *Nat. Mater.*, 2011, **10**, 74-80.
19. H. Yoshida, N. Yabuuchi and S. Komaba, *Electrochem. Commun.*, 2013, **34**, 60-63.
20. N. Yabuuchi, M. Kajiyama, J. Iwatate, H. Nishikawa, S. Hitomi, R. Okuyama, R. Usui, Y. Yamada and S. Komaba, *Nat. Mater.*, 2012, **11**, 512-517.
21. P. Vassilaras, A. J. Toumar and G. Ceder, *Electrochem. Commun.*, 2014, **38**, 79-81.
22. X. Sun, Y. Jin, C.-Y. Zhang, J.-W. Wen, Y. Shao, Y. Zang and C.-H. Chen, *J. Mater. Chem. A*, 2014, **2**, 17268-17271.
23. Y. Lei, X. Li, L. Liu and G. Ceder, *Chem. Mater.*, 2014, **26**, 5288-5296.
24. L. G. Chagas, D. Buchholz, C. Vaalma, L. Wu and S. Passerini, *J. Mater. Chem. A*, 2014, **2**, 20263-20270.
25. M. Sathya, K. Hemalatha, K. Ramesha, J. M. Tarascon and A. S. Prakash, *Chem. Mater.*, 2012, **24**, 1846-1853.
26. X. Wang, M. Tamaru, M. Okubo and A. Yamada, *J. Phys. Chem. C*, 2013, **117**, 15545-15551.
27. D. H. Lee, J. Xu and Y. S. Meng, *Phys. Chem. Chem. Phys.*, 2013, **15**, 3304-3312.
28. J. M. Paulsen and J. R. Dahn, *Solid State Ionics*, 1999, **126**, 3-24.
29. L. Dahéron, R. Dedryvère, H. Martinez, M. Ménétrier, C. Denage, C. Delmas and D. Gonbeau, *Chem. Mater.*, 2008, **20**, 583-590.
30. K. M. Shaju, G. V. Subba Rao and B. V. R. Chowdari, *Electrochim. Acta*, 2002, **48**, 145-151.
31. C. Gan, X. Hu, H. Zhan and Y. Zhou, *Solid State Ionics*, 2005, **176**, 687-692.
32. J.-H. Cheng, C.-J. Pan, J.-F. Lee, J.-M. Chen, M. Guignard, C. Delmas, D. Carlier and B.-J. Hwang, *Chem. Mater.*, 2014, **26**, 1219-1225.
33. V. Duffort, E. Talaie, R. Black and L. F. Nazar, *Chem. Mater.*, 2015, **27**, 2515-2524.
34. I. B. Hasa, D.; Passerini, S.; Scrosati, B., *Adv. Energy Mater.*, 2014, **4**, 1-7.
35. D. Yuan, W. He, F. Pei, F. Wu, Y. Wu, J. Qian, Y. Cao, X. Ai and H. Yang, *J. Mater. Chem. A*, 2013, **1**, 3895-3899.
36. S. Guo, P. Liu, H. Yu, Y. Zhu, M. Chen, M. Ishida and H. Zhou, *Angew. Chem. Int. Ed.*, 2015, **54**, 1-7.
37. Y. H. Jung, A. S. Christiansen, R. E. Johnsen, P. Norby and D. K. Kim, *Adv. Funct. Mater.*, 2015, **25**, 3227-3237.
38. Z. Lu and J. R. Dahn, *J. Electrochem. Soc.*, 2001, **148**, A1225.
39. Y. Li, Z. Yang, S. Xu, L. Mu, L. Gu, Y.-S. Hu, H. Li and L. Chen, *Adv. Sci.*, 2015, **2**, 2-7.
40. D. Su, C. Wang, H. J. Ahn and G. Wang, *Chem. Eur. J.*, 2013, **19**, 10884-10889.
41. X. Ma, H. Chen and G. Ceder, *J. Electrochem. Soc.*, 2011, **158**, A1307-A1312.

70

75

80

85

## Table of Contents

P-type layered oxide, biphasic, sodium-ion batteries,  $\text{Na}_{0.66}\text{Co}_{0.5}\text{Mn}_{0.5}\text{O}_2$ , high rate

5 Stable Layered P3/P2  $\text{Na}_{0.66}\text{Co}_{0.5}\text{Mn}_{0.5}\text{O}_2$  Cathode Materials for Sodium Ion Batteries

Xiaoqing Chen, Xianlong Zhou, Meng Hu, Jing Liang, Dihua Wu, Jinping Wei,\* Zhen Zhou\*

This work presents P3/P2-type biphasic layered  $\text{Na}_{0.66}\text{Mn}_{0.5}\text{Co}_{0.5}\text{O}_2$ , namely, integrating P2 into P3  
10 layered materials, and it delivered outstanding electrochemical performances.

